Citywide Assessment of Urban Tree Shading on Roof and Facade Solar Radiation Using Semantic 3D City Models

Markus Münzinger [1], Bruno Willenborg [2], Thomas H. Kolbe [2], Dirk Burghardt [3], Martin Behnisch [1 4]

[1] Leibniz Institute of Ecological Urban and Regional Development, 01217 Dresden, Germany
[2] Chair of Geoinformatics, TUM School of Engineering and Design, Technical University of Munich, 80333 Munich, Germany
[3] Chair of Cartographic Communication, [4] Chair of Spatial Information and Modelling, TU Dresden, 01069 Dresden, Germany
(m.muenzinger, m.behnisch)@ioer.de, (b.willenborg, thomas.kolbe)@tum.de, dirk.burghardt@tu-dresden.de

Keywords: Building Solar Radiation, Nature-based Solutions, Urban Trees, Semantic 3D City Models, Tree Shading

Abstract

Urban trees regulate solar radiation on building surfaces, influencing urban climate and energy performance. Using a semantic 3D city model, tree shading was quantified for all roofs and façades across the city of Munich, Germany. Solar irradiation was simulated for scenarios with and without trees using a tool supporting detailed 3D shadow analysis and urban-scale assessments, computing irradiation at 43 million points per scenario. Spatially explicit, surface-resolved shading effects were derived by comparing irradiation between the scenarios, isolating the impact of trees. Tree shading reduced annual global solar irradiation on buildings by 7 809 GWh (-11%). The reduction on facades (18%) was three times larger than on roofs. On roofs, direct and diffuse decreases balanced; facades showed a stronger drop in direct irradiation. Buildings taller than 15 m received only minor roof shading, while facade shading was measurable at all heights but diminished with increasing building height. Assessment of the vertical distribution of tree shading on facades revealed height-dependent reductions of 45–50% at ground level, 14–18% at 10 m, and ≈ 3% at 20 m; these values were consistent across different facade orientations. Nevertheless, south-facing facades consistently received higher absolute solar irradiance. These results quantify how tree shade varies with building morphology and provide a comprehensive overview of its cumulative impact across the city of Munich. The semantic structure of the 3D city model enables flexible aggregation and analysis down to individual building-envelope surfaces, a key added value that supports morphology-dependent assessments and informs the planning of sustainable and resilient urban environments.

1. Introduction

The modulation of solar radiation by urban trees at the building envelope represents a key mechanism linking climate adaptation and energy transition strategies in cities. Tree canopies reduce incoming shortwave radiation on roofs and facades, lowering surface temperatures, indoor heat gains, and cooling energy demand, while potentially limiting solar access for building-integrated photovoltaic (BIPV) systems (Balogun et al., 2014; Berry et al., 2013; Hsieh et al., 2018; Shen et al., 2026; Zhang et al., 2022). At the city-scale, aggregated shading contributes to Urban Heat Island mitigation and influences overall urban energy system performance (Czekajlo et al., 2023; Kim et al., 2025; Park et al., 2021).

This interaction places urban trees at the intersection of two major transformation domains. As Nature-based Solutions (NbS), trees provide regulating ecosystem services, particularly local climate regulation through shading and evapotranspiration, which improve thermal comfort, reduce heat stress, and enhance urban resilience (Guerry et al., 2023; Lwawa et al., 2022). Simultaneously, buildings are central to decarbonization efforts, with regulatory frameworks such as the European Energy Performance of Buildings Directive promoting energy efficiency and on-site renewable generation (European Union, 2024). Tree shading therefore directly links ecological adaptation (via NbS) with building-sector decarbonization, creating both synergies and trade-offs between reduced cooling demand and potential constraints on solar energy production. Managing urban trees therefore becomes an inherently interdisciplinary challenge, bridging ecology, urban planning, and energy systems. To support evidence-based decisions, planners and engineers require spatially explicit data that quantify both ecological benefits and energy-performance impacts (Ferrario et al., 2024; Menconi et al., 2026).

Although tree shading effects on solar radiation are well understood from detailed site-level urban climate simulations, studies that apply comparable detail at the city-scale remain limited. Citywide shading analyses (Aleksandrowicz et al., 2020; Park et al., 2023) and solar radiation assessments (Giannelli et al., 2022; Tian et al., 2023) that incorporate tree shading typically operate in 2.5D, representing rooftops or street-level surfaces and thereby neglecting vertical facades. True 3D simulations based on semantic 3D city models enable a detailed representation of building components and are increasingly used in solar radiation studies (Matsuoka et al., 2024; Willenborg et al., 2018a). By combining object-level geometry and hierarchical semantics, semantic 3D city models can also form the backbone of urban digital twins (Wysocki et al., 2024), enabling cities to be modelled with respect to their physical systems and environmental sustainability (Weil et al., 2022).

While buildings have traditionally been the focus, an increasing number of approaches now represent urban vegetation with the explicit goal of integrating it into semantic 3D city models (Ambarwari et al., 2024; Buyukdemircioglu and Oude Elberink, 2025; Münzinger et al., 2022), opening new possibilities for integrating tree shading into high-resolution city-scale simulations. At the building scale, studies by Peronato et al. (2016) and Willenborg et al. (2018b), on samples of 25 and 29 buildings respectively, have shown that shading from vegetation and other urban elements can substantially reduce solar radiation on facades, often more strongly than on roofs. Despite these advances, citywide, high-resolution 3D simulations that combine object-level accuracy with full spatial coverage remain scarce, leaving the cumulative impact of urban tree shading on solar radiation largely unquantified.

This study addresses this gap by quantifying the effects of urban tree shading on solar radiation at both roofs and facades across an entire city using semantic 3D city model simulations. Scenarios with and without trees were compared to provide spatially explicit, surface-level insights across the city, showing how tree canopies affect incident solar irradiance while accounting for building morphology, such as height and facade orientation. Furthermore, the approach provides a comprehensive overview of cumulative shading effects, thereby guiding planning for sustainable and resilient urban environments.

The remainder of the article is structured as follows. Section 2 describes the study area, the data, and the software used to model solar radiation. Section 3 outlines the methodology for assessing the shadow effect of trees. Section 4 presents and discusses the results of the comparative-scenario analysis. Section 5 concludes with a summary of the main findings and directions for future research.

2. Modelling Solar Irradiance in a Semantic 3D City Model

2.1 Study Area

The influence of tree shade on incoming solar irradiation was assessed for the entire building stock of Munich. Munich, with approximately 1.6 million inhabitants and an area of 311 km², is the third-largest city in Germany. The city is located on a broad, predominantly flat plateau in the northern Alpine foreland, approximately 50 km north of the Alps. Therefore, large-scale mountain shadow effects are likely negligible. Within the built-up area, the terrain is generally gentle, with no pronounced hills or major natural barriers, resulting in only minor topographic variation.

Munich exhibits a compact urban fabric with diverse building types and structures. The historic old town and the adjacent inner-city districts form a dense, mixed-use core. Surrounding this core, the outer districts are characterized by lower-rise residential blocks interspersed with commercial and office spaces. Most buildings are of low to medium height (< 30 m); consequently, shadow patterns are less complex than in high-rise cities.

Munich has an overall tree-canopy cover of 26%, slightly below the European average in urban areas (EEA, 2024). The city's urban forest is a mixture of deciduous and coniferous species, with deciduous trees predominating. In the context of building-related shading, the spatial distribution and composition of trees are particularly relevant. Almost half of Munich's trees are embedded within the built-up residential fabric, although tree density generally decreases with increasing building density (Leichtle et al., 2021).

2.2 Input Data

2.2.1 3D building model: For the present analysis, the official 3D building model supplied by the Bayerische Vermessungsverwaltung (LDBV) for 2019 was used. The semantic model corresponds to Level of Detail 2 (LoD 2) and is provided in CityGML format. It is based on officially surveyed building footprints and incorporates standardized roof forms derived from airborne LiDAR data and digital surface models. More detailed roof geometries, rooftop structures, and facade openings (doors and windows) are not included in the LoD 2 model. Geometric attributes, including surface area, height, and orientation, were calculated for each building surface. For the Munich urban area, the dataset comprises 286 293 buildings and ancillary structures such as bridges, walls, and canopies. These ancillary objects are treated as shading objects; however, solar-radiation analysis is performed only for the buildings. The modelled roof surface totals 46 km², and the facade surface totals 91 km².

2.2.2 3D tree model: A semantic 3D tree model for Munich, derived from airborne LiDAR point clouds collected in 2012 (Münzinger, 2025), was employed to simulate tree shading on building surfaces. The model represents reconstructed tree crowns as geometric primitives and conforms to CityGML LoD 2. For each tree, attributes such as height, crown diameter, and position were extracted from the LiDAR data. Implicit geometries were scaled individually to reproduce realistic crown volumes. The dataset includes all vegetation taller than 2 m, encompassing trees and shrubs, and comprises 2 364 638 modelled tree objects for the entire city. The individual objects have a mean height of 10 m, with the tallest object reaching 40 m.

The total count of tree objects should be regarded as an approximation, as automatic segmentation of individual trees from LiDAR data is prone to errors; particularly in complex or dense stands. Nevertheless, the reconstructed tree models provide a realistic representation of the urban forest. Tree crowns are modelled adaptively using parameterized geometric primitives, with dimensions derived from the LiDAR point cloud. Although segmentation errors occur and understory trees are largely omitted, the spatial distribution and volumetric structure of the urban forest are still well captured (cf. Münzinger et al., 2022).

2.3 Solar irradiation modelling

Solar irradiation for both scenarios was modelled with the software tool for solar potential assessment on semantic 3D city models presented by Willenborg et al. (2018a). The resulting dataset is publicly accessible via Zenodo (Willenborg et al., 2026a). The solar potential tool is available as Open Source Software (Willenborg et al., 2026b). It fetches the 3D city model from an instance of the 3D City Database 3DCityDB V4, see (Yao et al., 2018), and enriches the stored building objects and their parts by the calculated solar irradiation values. The tool supports detailed 3D simulations, including explicit shadow analysis and scalable large-area scenario evaluation, enabling urban-scale solar potential assessment. Validation against pyranometer measurements from the Deutscher Wetterdienst (DWD) confirmed that the tool provides reliable estimates for monthly and yearly aggregated solar irradiation, demonstrating its suitability for urban-scale solar potential assessments (Willenborg et al., 2018a).

The tool calculates direct and diffuse irradiation, while reflected irradiation is not included. Direct irradiation is calculated using the transition model developed by Fu and Rich (1999),

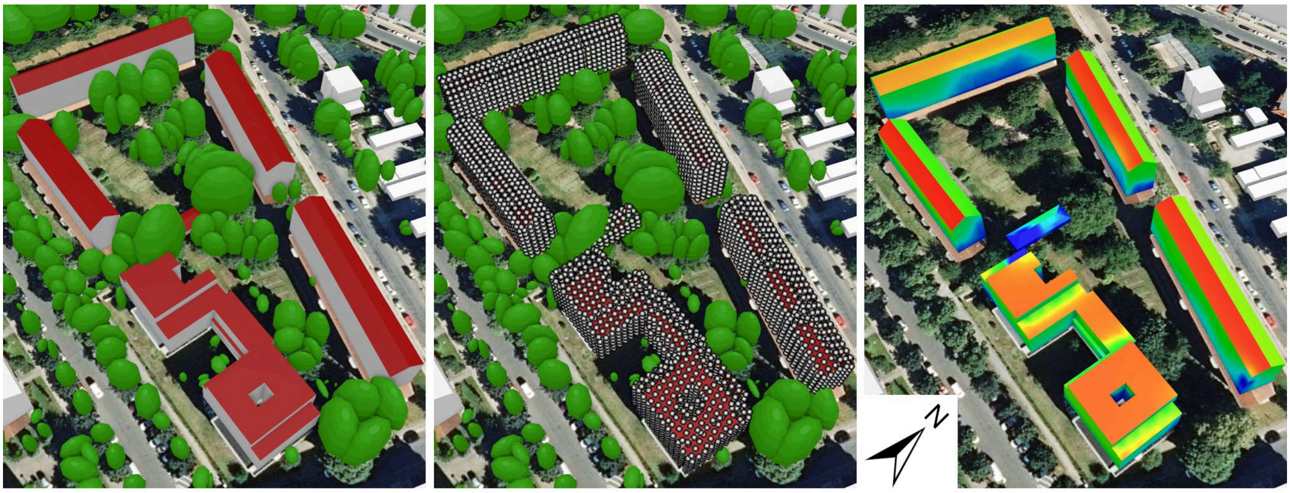

(a) (b) (c)

Figure 1: Exemplary illustration of the solar irradiation modelling workflow. (a) Input data: semantic 3D building model with roof surfaces (red) and facade surfaces (grey), as well as the 3D tree model (green). (b) Regular grid of sampling points generated on roof and facade surfaces. (c) Visualization of the annual global irradiation considering tree shading. Surface textures represent annual global irradiation values, with blue indicating low irradiation and red indicating high irradiation. Source data: Bayerische Vermessungsverwaltung, 2019, *www.geodaten.bayern.de*

accounting for solar position (Grena, 2012), intensity, and the orientation and inclination of each surface. Sun positions are computed throughout the year at hourly intervals, and the radiation power is adjusted for atmospheric transmissivity and optical path length. The transmissivity of the atmosphere and the fraction of diffuse irradiation in the global irradiation were calibrated using 22-year mean values from NASA Atmospheric Science Data Center data to ensure realistic estimates under long-term regional atmospheric conditions, while smoothing inter-annual variability. Shadowing was determined using a three-dimensional ray-tracing approach, casting rays from each surface point toward the sun based on a discretized hemispherical sky model. For the shadow analysis, surrounding buildings and trees were assumed to be fully opaque. Diffuse irradiation and the Sky View Factor (SVF) were derived from the same sky model, which represents the sky hemisphere using configurable azimuth and zenith divisions. The directional representation allows the contribution of obstructed sky regions and surface orientation to be considered in the diffuse irradiation calculation.

To model solar irradiation on roofs and facades, the official 3D building model of the City of Munich described above was applied. Terrain data derived from Digital Terrain Models and the 3D tree model were additionally integrated into the semantic 3D city model, allowing terrain and trees to be explicitly represented as shading objects (Fig. 1a). Each building roof and facade surface was discretized into a regular grid of points with 2 m point spacing, with each point representing a portion of the surface area. This discretization provides the reference locations for all irradiation computations. In total, around 43 million sampling points were used, approximately 12.6 million on roofs and 30.4 million on facades (Fig. 1b). Direct and diffuse solar irradiation, as well as the SVF, were computed at each surface point. Solar irradiation was computed in a regular temporal interval of 5 minutes over a full annual cycle. The modelling was carried out for two scenarios. In the first scenario, shading by the 3D tree model was included (Fig. 1c); in the second, tree shading was omitted. In both scenarios, shading from surrounding buildings and topography within a 100-m radius was modelled, while topographic shading was considered within a 20 km radius. Given the predominantly low- to medium-height buildings in the study area (< 30 m), this radius captures the relevant building- and tree-induced shading, as shadowing effects are dominated by nearby obstructions.

3. Methodology for Quantifying Tree-Shading Effects

The effect of tree-shading on solar irradiance of roofs and facades was quantified by contrasting two simulated scenarios, one with trees and one without. For each scenario, the model produced approximately 43 million sampling points. Every sampling point records the area it represents and the total incident irradiation, including both direct and diffuse components. Monthly irradiation values were aggregated temporally to obtain annual irradiation. Each sampling point is uniquely linked to a specific roof or facade surface and, through that surface, to its parent building in the semantic 3D building model. This relational structure enables flexible spatial aggregation at various thematic levels. For the subsequent analysis according to morphological building characteristics, each point was linked to the corresponding geometric attributes relevant for modelling solar radiation.

For the initial quantification of the overall impact of tree shading on roof and facade irradiation across the entire building stock, the annual irradiation components were aggregated separately for roofs and facades in both scenarios. Direct comparison of these aggregated values enabled the assessment of absolute and relative reductions in solar irradiation attributable to tree shading.

In a second step, shading effects were analysed in relation to building height. Annual specific solar irradiation (kWh/m²) was calculated for each roof and facade surface. The distribution of global annual irradiation across height classes and scenarios was examined using box-plots for both scenarios to assess differences in central tendency and variability. For facades, the analysis was evaluated under two configurations: (i) including all facades and (ii) including only non-north-facing facades, because north-facing facades in the Northern Hemisphere typically receive only negligible amounts of direct solar radiation. For the calculation of specific irradiation, only sampling points that received radiation in the no-tree scenario were included for facade surfaces. This procedure excluded wall areas permanently shaded by directly adjacent buildings, as such surfaces are not explicitly represented as separate entities in the LoD2 building model used in this study. Their inclusion would otherwise bias the results in densely built areas characterized by extensive shared wall sections. Building-height classes were adopted from the Global Human Settlement Layer (GHSL) height dataset (cf. Pesaresi et al., 2024).

In a third step, the vertical distribution of tree-induced shading along facades was examined in greater detail. Facade sampling points were classified into 1-m height intervals measured from ground level. Unlike the previous analysis, which used total building height, this step allowed a direct assessment of height-dependent shading patterns on the facade surface itself. The objective was to identify the height ranges at which trees produce the strongest reductions in direct solar irradiation. The analysis was limited to the vertical band from 0 to 20 m above ground. Annual specific direct irradiation (kWh/m²) was aggregated for each height interval and for each facade orientation; only non-north-facing facades were retained. The resulting vertical profiles of annual specific direct irradiation were visualized as heat maps, showing the height-dependent distribution of irradiation by orientation for both scenarios and the absolute reduction (Δ) attributable to tree shading.

The replication package, including all source code and data required to reproduce the analyses presented in this study, is publicly available (Münzinger et al., 2026).

4. Analysis of Tree Shading Effects

4.1 Overall Impact of Tree Shading on Roof and Facade Irradiation

Shading from urban trees reduced the annual global solar irradiation on all building surfaces by 7 809 GWh, representing an 11% decrease relative to the theoretical no-tree scenario (Table 1). The absolute reduction on roofs was 2 515 GWh (6% of the no-tree irradiation), whereas on facades it was 5 293 GWh (18% of the no-tree irradiation). Consequently, shading on vertical surfaces produced a markedly larger effect: the absolute reduction on facades was slightly more than twice that on roofs, and the relative reduction on facades was approximately three times larger than on roofs.

Further, the contributions of direct and diffuse irradiation components were examined. In the no-tree scenario, the direct component (≈ 36 TWh) exceeded the diffuse component (≈ 32 TWh). When expressed as a share of the total incident irradiation, diffuse irradiation accounted for roughly 46% of the annual total on roofs and 49% on facades. On roofs, the reductions were comparable for direct and diffuse irradiation (approximately 7% and 6%, respectively). On facades, direct irradiation was reduced more strongly than diffuse irradiation (25% versus 11%). While in the no-tree scenario the ratio between diffuse and direct irradiation was balanced, inclusion of tree shading reduced the direct component by 3 695 GWh and the diffuse component by 1 599 GWh, thereby increasing the diffuse share on facades. Two conclusions can be drawn regarding the effect of tree shading on buildings. Roofs, being horizontal or inclined, receive a mixture of direct and sky-diffuse irradiation from a wide range of solar elevations; consequently, the tree canopy shades a similar proportion of both components. Conversely, tree crowns intercept a larger fraction of the low-angle direct beam that strikes vertical surfaces, making the diffuse component the dominant contributor of facade irradiation.

Com-ponent	Sur-face	No Tree Shade (GWh)	Tree Shade (GWh)	Δ %	Δ GWh
Global	Roof	39 526	37 011	6.4	2 515
	Facade	28 776	23 482	18.4	5 294
	Total	**68 302**	**60 493**	**11.4**	**7 809**
Direct	Roof	21 329	19 903	6.7	1 426
	Facade	14 558	10 863	25.4	3 695
	Total	**35 887**	**30 766**	**14.3**	**5 121**
Diffuse	Roof	18 197	17 107	6.0	1 089
	Facade	14 217	12 619	11.2	1 599
	Total	**32 414**	**29 726**	**8.3**	**2 688**

Table 1: Annual solar irradiation on roof and facade surfaces under two shading scenarios. No-Tree-Shading represents the theoretical maximum. Tree-Shading incorporates the effect of existing trees and is therefore the most realistic estimate.

The citywide analysis of the overall impact of tree shading, covering a variety of building sizes and forms, shows how strong tree shading reduces incoming solar irradiation. Omitting trees from urban-scale solar-irradiance models leads to a systematic over-estimation of the energy received, especially on facades, where the reduction in the direct component is most pronounced.

4.2 Influence of Building Height on Specific Solar Irradiation

To examine the building stock in greater detail, shading impacts were analysed in relation to building height. Differences in the distribution of annual specific irradiation between the two scenarios were evaluated for separate height classes and for roofs and facades independently, using box-plots (Fig. 2).

The no-tree-shading scenario was used as the baseline. In this scenario, the interquartile range (IQR) of global irradiation differed markedly between roofs and facades: for roofs, the IQR spanned roughly 540–1015 kWh/m², whereas the IQR for facades covered 200–470 kWh/m² for all orientations and 285–580 kWh/m² for the non-north-facing facades. Apart from these range differences, the overall shape of the distributions was similar across height classes. In this baseline scenario, two counterintuitive observations emerged. First, the lowest roof irradiation values occurred in the tallest building height class (> 30 m). Buildings were classified by their overall height; therefore, this class would normally be expected to contain the highest and least obstructed roof surfaces. However, it also included many complex buildings (e.g., churches) with lower attached roof sections below the main structure, which are often shaded by higher parts of the same building. Second, for facades, the highest irradiation values were recorded for buildings in the 6–15 m height class in both configurations. Here as well, the highest values might have been expected for the tallest facades. However, this height range comprised many detached single-family houses as well as free-standing industrial and commercial halls, which are generally situated in less densely built-up areas.

Comparison with the tree-shading scenario indicated that roof shading was pronounced primarily for buildings lower than 15 m, with the strongest effect in the low-rise classes (< 6 m). Median reductions in specific annual irradiation were 241 kWh/m² for roofs < 3 m, 201 kWh/m² for roofs 3–6 m, and 80 kWh/m² for the 6–15 m class; for buildings > 15 m only minor median differences of 12 kWh/m² and 10 kWh/m² were observed. The

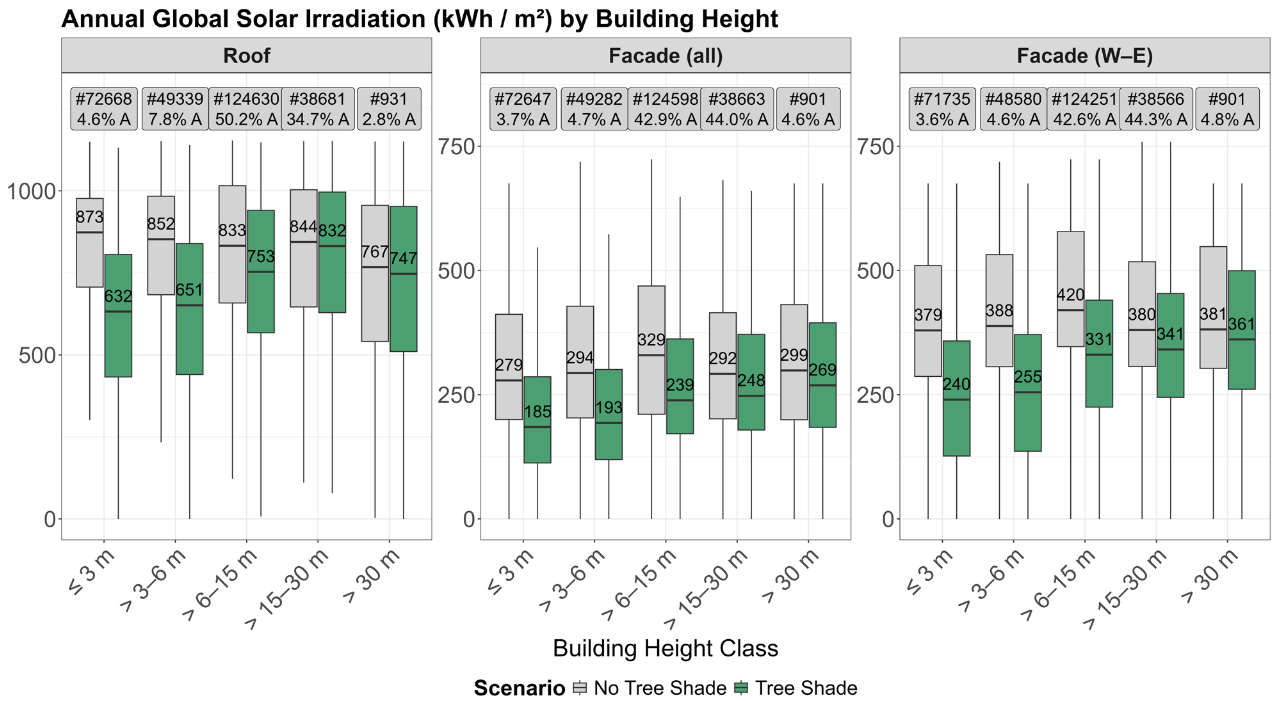

Figure 2: Distribution of annual specific solar irradiation across building height classes for roofs and facades in both scenarios. For facades, two configurations are shown: (all) all facades and (W-E) only non-north-facing facades. Labels indicate the number of buildings and their share of total roof or facade area in each height class.

analysis of facade irradiation showed a reduction in the value distributions for every height class, with the greatest reduction occurring for low-rise buildings. Across all facades, median irradiation in the tree-shading scenario was approximately 100 kWh/m² lower than in the no-tree scenario; for facades without a north-facing component the median reduction was roughly 140 kWh/m². For taller buildings, a comparable magnitude of reduction was observed in both facade categories. In the 6–15 m height class the median difference between scenarios was about 90 kWh/m², and for the upper height classes the reduction became smaller, with median differences of roughly 40 kWh/m² for all facades and 30 kWh/m² for the non-north-facing facades.
By relating the measured irradiation to building height, the strong dependence of tree-induced shading on urban morphology was evident. Although only 39 613 of the 286 293 buildings (≈ 14%) exceeded 15 m, they accounted for 37.5% of the modelled roof area because taller buildings generally possess larger roofs. Consequently, the observed 6% reduction in total roof irradiation must be interpreted in light of the fact that the majority of roof surface lies at heights where tree shade is scarce. For facades, the effect of tree shading was more nuanced. Since facades extend from the eaves to ground level, every building, irrespective of height, contains lower-lying facade sections that were exposed to tree shade. Nevertheless, the analysis showed a clear trend: the higher the building, the smaller the impact of shading on the facade-irradiation distribution, because an increasing proportion of the facade area lies above the reach of tree crowns and therefore remains unshaded.

When interpreting the presented values of annual solar irradiation on roofs and facades, several factors should be considered, as these values are partially lower than the maximal potential reported by other sources. The modelling tool slightly underestimates annual irradiation compared to DWD pyranometer measurements, with a systematic underestimation of ~3% per year (Willenborg et al., 2018a). Seasonal biases further affected the results: direct irradiation is underestimated during summer, when solar angles are high, and overestimated in winter, with the summer underestimation having a greater impact on annual totals. In addition, reflected radiation from surrounding surfaces was omitted, which would otherwise increase especially facade values. Furthermore, all roof and facade surfaces were included irrespective of orientation or roof slope, capturing areas with lower irradiation. Despite these generally lower absolute values, the relative reductions due to tree shading remain consistent, indicating that the comparative effects are robust.

4.3 Vertical Distribution of Tree Shading Effects

To further examine the modelled shading effects on facades, a detailed height-dependent analysis was conducted using heat maps showing annual specific direct irradiation by facade orientation and relative height above ground (Fig. 3a).
In the theoretical no-tree scenario, a dominant influence of facade orientation on incoming irradiation was revealed, whereas relative height above ground within each orientation class had a comparatively minor impact. West- and east-facing facades received maximum direct irradiation of 189 kWh/m² and 183 kWh/m², respectively, at heights above 15 m. Near ground level, shading by adjacent buildings and topography lowered these values to 155 kWh/m² and 154 kWh/m², a height-related reduction of about 17%. South-facing facades exhibited the highest values, reaching up to 439 kWh/m² above 15 m. At low height, direct irradiation on south-facing facades was roughly 85 kWh/m² lower than on higher sections, corresponding to a 20% difference. Thus, when tree shading was not considered, facade orientation had a stronger impact on incoming solar irradiation than building height.

When tree shading was incorporated, the pattern that had previously been dominated by facade orientation changed markedly (Fig. 3b). The lower portions of facades experienced the greatest reductions because they were most exposed to

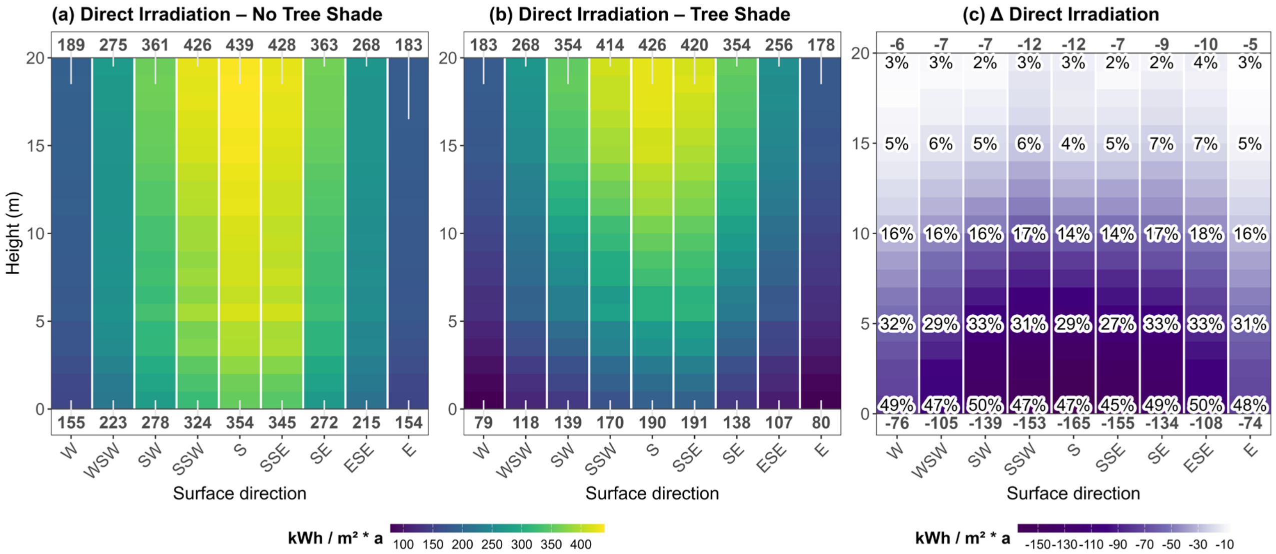

Figure 3: Heat maps of vertical profiles of annual direct irradiation. Min and max values for each bar are labelled, with lines indicating the corresponding cells. (a) No-tree shading scenario. (b) Tree-shading scenario. (c) Difference (Δ) with relative reduction per orientation and height labelled.

shadows cast by surrounding trees. The largest absolute decrease was observed on south-facing facades near ground level, where irradiation fell by 165 kWh/m², a reduction of 47% relative to the no-tree scenario. The height-dependent reduction was comparable across all facade orientations (Fig. 3c). Relative decreases in direct irradiation were 45–50% at ground level, 27–33% at 5 m, 14–18% at 10 m, about 5% at 15 m, and roughly 3% at 20 m. Although south-facing facades showed larger absolute reductions because they receive more irradiation, the decreasing trend with height was consistent for every orientation.

This high-resolution assessment demonstrates the analytical depth enabled by the modelling approach. Unlike the previous aggregation at roof or facade level, the analysis was conducted directly at the level of individual sampling points and linked to their corresponding facade surfaces within the semantic hierarchy of the model. The results confirmed the dominant influence of facade orientation on theoretical irradiation potential. In the no-tree scenario, south-facing facades showed substantially higher annual specific direct irradiation than west- or east-facing facades. Despite these orientation-driven differences in absolute values, the relative reduction in direct irradiation due to tree shading was largely consistent across height intervals. This indicates that tree-induced shading affected facades along their height in a comparatively uniform manner within the analysed range.

5. Conclusions

Using a semantic 3D city model, this study quantified the shading effect of urban trees on roofs and facades across an entire city. High-resolution solar irradiance mapping, based on a dense grid of 43 million sampling points, enabled a comparison of two scenarios, with and without trees, revealing the cumulative impact of tree shading on citywide solar radiation patterns. The results highlight citywide trends in shading, identify potential deficits, and provide a basis for analysing the trade-offs associated with tree-induced shading, which simultaneously affects energy performance through reduced solar irradiation availability for renewable energy generation and provides ecological benefits through local climate regulation. By leveraging the hierarchical structure of the semantic 3D city model, each sampling point is linked to its roof or façade and to the parent building, allowing surface- and building-level analyses that reveal how shading depends on building form and orientation. These insights offer practical guidance for strategic urban forest management and the design of sustainable, resilient cities.

By quantifying an 11% overall decrease, and an 18% reduction on vertical surfaces, this study demonstrates that trees must be explicitly represented in urban simulations to avoid biased assessments of solar exposure and to support realistic planning of sustainable, resilient cities. Analysis of building morphology shows that roofs generally receive higher irradiance than facades, making elevated roof surfaces less affected by tree shading and highlighting areas with high potential for rooftop photovoltaic deployment. At the same time, the strongest shading occurs on lower facade sections, showing that trees can effectively reduce thermal loads on buildings and surrounding streets, contributing to Urban Heat Island mitigation. The results also make visible the heights at which tree shading is most relevant, providing important guidance for combining solar energy strategies with vegetation, for example, identifying areas where elevated roofs could maximize energy gain while lower facades benefit from cooling, or BIPV can serve dual purposes as energy generators and shading devices.

Several avenues remain for refinement and extension. The shading effects are likely slightly overestimated, as trees were modelled as fully opaque; however, even partial shading can significantly affect surface warming and the performance of photovoltaic systems. In addition, no distinction was made between tree species, which can influence shading patterns and seasonal dynamics. The seven-year temporal mismatch between the building and tree datasets may introduce inconsistencies in areas with construction activities or vegetation changes. While acceptable for a city-wide assessment, future analyses would benefit from temporally consistent input datasets. The study analysed annual solar irradiation, but examining specific months, such as summer, with high irradiance and varying sun angles, could provide additional seasonal insights. Further analyses, stratified according to urban morphology, could reveal how spatial configurations amplify or reduce shading effects and make explicit interactions that are already implicitly represented in the semantic 3D city model. Finally, while this study focuses on the status quo, the same framework could be applied to future scenarios with variations in tree cover or building stock, supporting planning for shading, solar radiation, and sustainable urban development.

Overall, the study demonstrates the added value of integrating trees into semantic 3D city models: such detailed representations provide a critical foundation for urban digital twins, enabling planners and engineers to quantify both ecological benefits and energy-performance impacts in a spatially explicit, policy-relevant, decision-support framework.

Acknowledgements

The authors acknowledge the use of modeling results generated within the *StandardBIPV* project (FKZ 0324063C), funded by the German Federal Ministry for Economic Affairs and Energy (BMWi), as well as the provision of geospatial data by the Bavarian Surveying Administration within the project *Anwendungen mit Geomassendaten* of Runder Tisch GIS e.V..

References

Aleksandrowicz, O., Zur, S., Lebendiger, Y., Lerman, Y., 2020. Shade maps for prioritizing municipal microclimatic action in hot climates: Learning from Tel Aviv-Yafo. *Sustainable Cities and Society*, 53, 101931. https://doi.org/10.1016/j.scs.2019.101931

Ambarwari, A., Suwardhi, D., Rani, M.S., Husni, E., Junaidy, D.W., Agirachman, F.A., Murtiyoso, A., Griess, V.C., 2024. Conceptual Model of Graph-based Individual Tree and Its Utilization in Digital Twin and Metaverse of Urban Forest. *Int. Arch. Photogramm. Remote Sens. Spatial Inf. Sci.,* XLVIII-4–2024, 7–12. https://doi.org/10.5194/isprs-archives-XLVIII-4-2024-7-2024

Balogun, A.A., Morakinyo, T.E., Adegun, O.B., 2014. Effect of tree-shading on energy demand of two similar buildings. *Energy and Buildings*, 81, 305–315. https://doi.org/10.1016/j.enbuild.2014.05.046

Berry, R., Livesley, S.J., Aye, L., 2013. Tree canopy shade impacts on solar irradiance received by building walls and their surface temperature. *Building and Environment*, 69, 91–100. https://doi.org/10.1016/j.buildenv.2013.07.009

Buyukdemircioglu, M., Oude Elberink, S., 2025. Enriching Urban Digital Twins with Energy-related Information from Aerial and Street View Imagery for Precise Urban Climate Modeling. *Int. Arch. Photogramm. Remote Sens. Spatial Inf. Sci.*, XLVIII-M-6–2025, 79–85. https://doi.org/10.5194/isprs-archives-XLVIII-M-6-2025-79-2025

Czekajlo, A., Alva, J., Szeto, J., Girling, C., Kellett, R., 2023. Impact of 2050 tree shading strategies on building cooling demands. *Buildings and Cities*, 4, 817–837. https://doi.org/10.5334/bc.353

European Environment Agency (EEA), 2024. Urban tree cover dashboard. https://www.eea.europa.eu/en/analysis/maps-and-charts/urban-tree-cover-dashboard. (05 March 2026).

European Union, 2024. Directive (EU) 2024/1275 of the European Parliament and of the Council of 24 April 2024 on the energy performance of buildings (recast).

Ferrario, F., Mourato, J.M., Rodrigues, M.S., Dias, L.F., 2024. Evaluating Nature-based Solutions as urban resilience and climate adaptation tools: A meta-analysis of their benefits on heatwaves and floods. *Science of The Total Environment*, 950, 175179. https://doi.org/10.1016/j.scitotenv.2024.175179

Fu, P. and Rich, P.M., 1999. Design and implementation of the Solar Analyst: an ArcView extension for modeling solar radiation at landscape scales. *Proceedings of the Nineteenth Annual ESRI User Conference*

Giannelli, D., León-Sánchez, C., Agugiaro, G., 2022. Comparison and Evaluation of Different GIS Software Tools to Estimate Solar Irradiation. *ISPRS Ann. Photogramm. Remote Sens. Spatial Inf. Sci.*, V-4–2022, 275–282. https://doi.org/10.5194/isprs-annals-V-4-2022-275-2022

Grena, R., 2012. Five new algorithms for the computation of sun position from 2010 to 2110. *Solar Energy*, 86, 1323–1337. https://doi.org/10.1016/j.solener.2012.01.024

Guerry, A.D., Lonsdorf, E.V., Nootenboom, C., Remme, R.P., Griffin, R., Waters, H., Polasky, S., Han, B., Wu, T., D. Janke, B., Meacham, M., Hamel, P., Wang, X., 2023. Mapping, measuring, and valuing the benefits of nature-based solutions in cities, in: McPhearson, T., Kabisch, N., Frantzeskaki, N. (Eds.), *Nature-Based Solutions for Cities*. Edward Elgar Publishing, pp. 259–293. https://doi.org/10.4337/9781800376762.00023

Hsieh, C.-M., Li, J.-J., Zhang, L., Schwegler, B., 2018. Effects of tree shading and transpiration on building cooling energy use. *Energy and Buildings*, 159, 382–397. https://doi.org/10.1016/j.enbuild.2017.10.045

Kim, S.H., Ku, B., Park, C.Y., Aida, A., Cheng, H., Kim, S., Park, C., 2025. Quantifying the average cooling effects of tree, artificial, and hybrid shade using city-wide IoT sensor measurements: A case study of Seoul. *Sustainable Cities and Society*, 133, 106855. https://doi.org/10.1016/j.scs.2025.106855

Leichtle, T., Zehner, M., Kühnl, M., Martin, K., Taubenböck, H., 2021. Urban trees–detection, delineation, quantification, and characterisation based on vhr remote sensing. *Proceedings of the REAL CORP 2021*, 1029-1039. https://elib.dlr.de/143807/

Lwawa, S., Seto, K.C., Bai, X., Blanco, H., Gurney, K.R., Kılıṣ, Ş., Lucon, O., Murakami, J., Pan, J., Sharifi, A., Yamagata, Y., 2022. Urban systems and other settlements, in: Shukla, P.R., Skea, J., Slade, R., Al Khourdajie, A., van Diemen, R., McCollum, D., Pathak, M., Some, S., Vyas, P., Fradera, R., Belkacemi, M., Hasija, A., Lisboa, G., Luz, S., Malley, J. (Eds.), *Climate Change 2022: Mitigation of Climate Change. Contribution of Working Group III to the Sixth Assessment Report of the Intergovernmental Panel on Climate Change*. Cambridge University Press, Cambridge, UK and New York, NY, USA, 861–952. https://doi.org/10.1017/9781009157926.010

Matsuoka, R., Takemoto, T., Takahashi, G., Inazawa, T., Sogo, S., 2024. Estimation of Photovoltaic Potential of Urban Buildings Considering a Solar Panel Arrangement Using a 3D City Model. *ISPRS Annals of the Photogrammetry, Remote Sensing and Spatial Information Sciences*, X-4-W4-2024, 123–130. https://doi.org/10.5194/isprs-annals-X-4-W4-2024-123-2024

Menconi, M., Vizzari, M., Grohmann, D., 2026. Optimizing local regulating ecosystem services through nature-based urban retrofitting scenarios. *Ecosystem Services*, 77, 101805. https://doi.org/10.1016/j.ecoser.2025.101805

Münzinger, M., Willenborg, B., Kolbe, T.H., Burghardt, D., Behnisch, M., 2026. Replication Package for: Citywide Assessment of Urban Tree Shading on Roof and Facade Solar Radiation Using Semantic 3D City Models [Data set]. ioerDATA, V1. https://doi.org/10.71830/6PHWRQ

Münzinger, M., 2025, LiDAR-Based Tree Models for Munich, Germany (2012) [Data set]. ioerDATA, V1. https://doi.org/10.71830/NDTUDB

Münzinger, M., Prechtel, N., Behnisch, M., 2022. Mapping the urban forest in detail: From LiDAR point clouds to 3D tree models. *Urban Forestry & Urban Greening*, 74, 127637. https://doi.org/10.1016/j.ufug.2022.127637

Park, Y., Guldmann, J.-M., Liu, D., 2021. Impacts of tree and building shades on the urban heat island: Combining remote sensing, 3D digital city and spatial regression approaches. *Computers, Environment and Urban Systems*, 88, 101655. https://doi.org/10.1016/j.compenvurbsys.2021.101655

Park, Y., Zhao, Q., Guldmann, J.-M., Wentz, E.A., 2023. Quantifying the cumulative cooling effects of 3D building and tree shade with high resolution thermal imagery in a hot arid urban climate. *Landscape and Urban Planning*, 240, 104874. https://doi.org/10.1016/j.landurbplan.2023.104874

Peronato, G., Rey, E., Andersen, M., 2016. 3D Modeling of Vegetation from LIDAR Point Clouds and Assessment of Its Impact on Façade Solar Irradiation. *Int. Arch. Photogramm. Remote Sens. Spatial Inf. Sci.*, XLII-2-W2, 67–70. https://doi.org/10.5194/isprs-archives-XLII-2-W2-67-2016

Pesaresi, M., Schiavina, M., Politis, P., Freire, S., Krasnodębska, K., Uhl, J.H., Carioli, A., Corbane, C., Dijkstra, L., Florio, P., Friedrich, H.K., Gao, J., Leyk, S., Lu, L., Maffenini, L., Mari-Rivero, I., Melchiorri, M., Syrris, V., Van Den Hoek, J., Kemper, T., 2024. Advances on the Global Human Settlement Layer by joint assessment of Earth Observation and population survey data. *International Journal of Digital Earth*, 17, 2390454. https://doi.org/10.1080/17538947.2024.2390454

Shen, Z., Qi, F., Zhang, T., Song, Y., Zhou, Y., 2026. A calculation method for indoor solar irradiance under tree shading. *Solar Energy*, 305, 114282. https://doi.org/10.1016/j.solener.2025.114282

Tian, B., Loonen, R.C.G.M., Hensen, J.L.M., 2023. Combining point cloud and surface methods for modeling partial shading impacts of trees on urban solar irradiance. *Energy and Buildings*, 298, 113420. https://doi.org/10.1016/j.enbuild.2023.113420

Weil, C., Bibri, S.E., Longchamp, R., Golay, F., Alahi, A., 2023. Urban Digital Twin Challenges: A Systematic Review and Perspectives for Sustainable Smart Cities. *Sustainable Cities and Society*, 99, 104862. https://doi.org/10.1016/j.scs.2023.104862

Willenborg, B., Münzinger, M., Behnisch, M., & Kolbe, T. H., 2026a. 3D Solar Potential Analysis Results for Munich based on CityGML Semantic City Models (1.0.0) [Data set]. Zenodo. https://doi.org/10.5281/zenodo.19192862

Willenborg, B., Sindram, M., Kolbe, T. H., 2026b. The 3DCityDB v4 Solar Irradiation and Sky View Factor Calculator [Data set]. https://doi.org/10.5281/zenodo.21334118

Willenborg, B., Sindram, M., Kolbe, T.H., 2018a. Applications of 3D City Models for a Better Understanding of the Built Environment, in: Behnisch, M., Meinel, G. (Eds.), *Trends in Spatial Analysis and Modelling, Geotechnologies and the Environment*. Springer International Publishing, Cham, pp. 167–191. https://doi.org/10.1007/978-3-319-52522-8_9

Willenborg, B., Pültz, M., Kolbe, T.H., 2018b. Integration of Semantic 3D City Models and 3D Mesh Models for Accuracy Improvements of Solar Potential Analyses. *Int. Arch. Photogramm. Remote Sens. Spatial Inf. Sci.*, XLII-4-W10, 223–230. https://doi.org/10.5194/isprs-archives-XLII-4-W10-223-2018

Wysocki, O., Schwab, B., Beil, C., Holst, C., Kolbe, T.H., 2024. Reviewing Open Data Semantic 3D City Models to Develop Novel 3D Reconstruction Methods. *Int. Arch. Photogramm. Remote Sens. Spatial Inf. Sci.*, XLVIII-4–2024, 493–500. https://doi.org/10.5194/isprs-archives-XLVIII-4-2024-493-2024

Yao, Z., Nagel, C., Kunde, F., Hudra, G., Willkomm, P., Donaubauer, A., Adolphi, T., Kolbe, T. H., 2018. 3DCityDB - a 3D geodatabase solution for the management, analysis, and visualization of semantic 3D city models based on CityGML. *Open Geospatial Data, Software and Standards*, 3, 5. https://doi.org/10.1186/s40965-018-0046-7

Zhang, T., Spence, C., Qi, F., Yang, W., Song, T., 2022. Influence of tree location on thermal radiation disturbance of the west wall of summer buildings. *Energy and Buildings*, 273, 112359. https://doi.org/10.1016/j.enbuild.2022.112359

Zhao, Y., Chen, Y., Li, K., 2022. A simulation study on the effects of tree height variations on the façade temperature of enclosed courtyard in North China. *Building and Environment*, 207, 108566. https://doi.org/10.1016/j.buildenv.2021.108566